ACS APPLIED MATERIALS & INTERFACES

Research Article

www.acsami.org

Mechanochemistry at Solid Surfaces: Polymerization of Adsorbed Molecules by Mechanical Shear at Tribological Interfaces

Jejoon Yeon,[†,§] Xin He,[‡,§] Ashlie Martini,[†] and Seong H. Kim*[,‡]

[†]School of Engineering, University of California, Merced, California 95343, United States

[‡]Department of Chemical Engineering and Materials Research Institute, Pennsylvania State University, University Park, Pennsylvania 16802, United States

Supporting Information

ABSTRACT: Polymerization of allyl alcohol adsorbed and sheared at a silicon oxide interface is studied using tribo-tests in vapor phase lubrication conditions and reactive molecular dynamics simulations. The load dependences of product formation obtained from experiments and simulations were consistent, indicating that the atomic-scale processes observable in the simulations were relevant to the experiments. Analysis of the experimental results in the context of mechanically assisted thermal reaction theory, combined with the atomistic details available from the simulations, suggested that the association reaction pathway of allyl alcohol molecules induced by mechanical shear is quite different from chemically induced polymerization reactions. Findings suggested that some degree of distortion of the molecule from its equilibrium state is necessary for mechanically induced chemical reactions to occur and such a distortion occurs during mechanical shear when molecules are covalently anchored to one of the sliding surfaces.

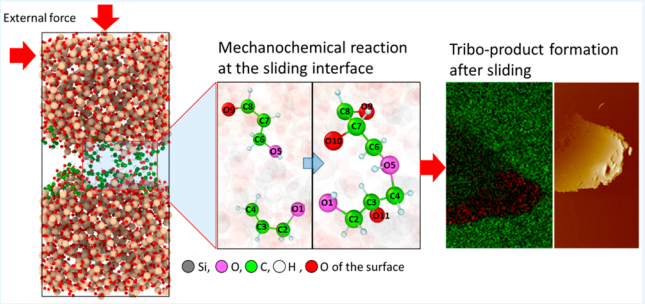

KEYWORDS: *mechanochemistry, tribology, shear-induced chemical reactions, ReaxFF MD simulations, vapor phase lubrication*

INTRODUCTION

Mechanochemical reactions are ubiquitous, but often unnoticed or considered atypical. An example of mechanochemistry is a chemical reaction that occurs at the sliding interface of two solid materials, often called tribochemical reactions.[1−3] Another example is synthesis of organic chemicals by collision of solid particles as in ball milling processes.[4−7] These reactions are quite different from chemical reactions that occur upon heating, photon irradiation, or electrical bias. In thermochemistry, thermal excitation of molecules drives electrons in the ground state to go through a transition state along a specific reaction coordinate. The energy difference between the ground and transition states is called an activation barrier; this barrier could be lowered by using a proper catalyst to accelerate the chemical reaction rate. In photochemistry, the absorption of photons leads to excitation of electrons from the ground state to an excited state followed by propagation or relaxation of the excited electronic state to a lower energy state which is different from the initial state. In electrochemistry, transfer of electrons from an oxidizing species to a reducing species takes place when electrical contact is made between two reacting species with different electrochemical potentials; such redox reactions can be facilitated by application of electrical potential or bias. In contrast to these chemical reactions, where the transition or flow of electrons between electronic states leads to changes in atomic positions of molecules involved in reactions, a mechanistic understanding of mechanochemical reactions, in which a mechanical force alters reaction energies and pathways, is not well established. In this work, we are specifically interested in how mechanical force or stress can be transferred to molecules from external solid surfaces, displacing the molecular conformation from equilibrium states or positions, and how that can lead to chemical reactions involving changes in electronic states of reacting species.

At tribological interfaces, frictional energy can induce a significant increase in temperature, especially when the friction and sliding speed are high; such frictional heat can induce thermal reactions.[8] When solid surfaces wear or fracture, high-energy particles such as electrons or photons can be emitted. These are called triboplasma and triboemission.[9,10] Then, electrochemical or photochemical reactions can be accompanied. It is known that tribochemical reactions can take place even without substantial frictional heat or surface wear and fracture.[11−13] In this case, external mechanical force or energy is assumed to be directly channeled into reaction coordinates, inducing distortion or dissociation of molecules. In such cases, the reaction rate or yield increases exponentially with the applied force or energy.[14,15] This is often modeled as a mechanically assisted thermal reaction where the mechanical energy is effectively lowering the activation barrier; thus,

Received: November 4, 2016
Accepted: December 27, 2016
Published: December 27, 2016

DOI: 10.1021/acsami.6b14159
ACS Appl. Mater. Interfaces 2017, 9, 3142−3148

the reaction rate (r_p) or yield (r_y) can be expressed in the following Arrhenius-type equation:[14,15]

$$r_y = A \exp\left(-\frac{E_a - \Delta x^* F}{k_B T}\right) = A \exp\left(-\frac{E_a - \sigma \Delta V^*}{k_B T}\right) \quad (1)$$

where A is the preexponential factor, k_B the Boltzmann constant, and T the system temperature; here, the mechanical energy term is expressed as $\Delta x^* F$ at a given applied force or $\sigma \Delta V^*$ at a given contact stress and counteracts the thermal activation barrier (E_a).[12−17] In this context, the mechanical effect can be viewed as *equivalent to* the catalysis effect because it lowers the reaction barrier. In eq 1, the proportionality constants, Δx^* and ΔV^*, are called "critical activation distance" and "critical activation volume", respectively, based on the dimensional analysis. However, their exact physical meaning is still unclear.

Theoretically, it was shown that the dissociation channel of the Morse potential of a chemical bond can bend down under the influence of external force (F).[18−20] In that case, an energy maximum point occurs at a distance Δx^* away from the equilibrium bond distance (x_e).[19] The energy at $x_e + \Delta x^*$ is much lower than the equilibrium bond energy (E_b); thus, bond dissociation can occur at a temperature much lower than typical thermal reaction temperatures. Experimentally, ΔV^* can be obtained from the dependence of reaction yield or rate on contact pressure or shear stress (σ).[12,14,16,21] Although, the magnitude of ΔV^* can be determined experimentally, its physical meaning related to mechanistic pathways is still ambiguous.

In order to obtain a mechanistic understanding of mechanical activation of chemical reactions, this work integrated experimental and computational studies of tribo-polymerization of allyl alcohol adsorbed at a sliding interface of silicon oxide. Experimental tribo-tests were conducted in a vapor phase lubrication (VPL) condition where frictional heat generation as well as surface wear are negligible (see sections I and II of the Supporting Information);[11,22,23] thus, heat-, plasma-, and radiation-induced pathways are insignificant. Since silicon oxide is an insulator, electrochemical pathways can be ruled out. Computational molecular dynamics (MD) simulations were performed using a reactive force field called ReaxFF which can handle a sufficiently large number of atoms and molecules under dynamic and reactive environments.[24−28] We verified that ReaxFF MD simulation results are relevant to the experimental data by comparing the slopes of the $\ln(r_y)$ vs contact pressure (P) plot from the experiment and the $\ln(r_p)$ vs P plot from the simulation results. Note that the magnitude of A in eq 1 varies depending on whether r_p or r_y is plotted, since conversion of r_y to r_p requires multiplication by additional parameters; but this does not alter the Arrhenius slope of the pressure dependence. MD simulations revealed the dominant reaction pathway for the association of allyl alcohol induced by mechanical shear, which is quite different from typical radical-based polymerization reactions. The physical meaning of the magnitude of ΔV^* is discussed based on the computation results.

METHODS

Tribo-polymerization of allyl alcohol at a sliding interface of silicon oxide was studied using a ball-on-flat tribometer capable of environmental control during friction testing.[23] The substrate was thermally grown oxide layers on a silicon wafer and the counter surface was sodium borosilicate glass balls (Pyrex, thermal expansion coefficient = 3.3 ppm/K; diameter = 2.38 mm). Borosilicates balls were used for the most of the experimental tests after confirming that the product yields obtained with silica balls and borosilicate balls were similar at one loading condition. The use of borosilicate balls instead of silica balls was mainly because the former have much smoother surface, which eliminates or reduces asperity contact issues. Note that both borosilicate and silica balls show similar wear behaviors in dry and n-alcohol VPL conditions.[22,29] The sliding track and ball surfaces were analyzed with optical profilometry (Zygo NewView 7300) after the tribo-test and no wear was observed. Due to surface charging problems, scanning electron microscopy (SEM) analysis for detection of microcracks smaller than the resolution of optical profilometry was not carried out. Even if there were a few microcracks detectable at the SEM resolution, their total surface area would be much smaller than the contact area (especially, in the absence of wear). Thus, the effect of microcracks on total reaction yields would be insignificant.

Tribo-polymer production yield was measured with atomic force microscopy (AFM) (Digital Instrument, MultiMode). Tribo-polymer products were analyzed with X-ray photoelectron spectroscopy (XPS) (PHI, VersaProbe) (see section III in the Supporting Information) and time-of-flight secondary ion mass spectrometry (ToF-SIMS) (PHI, TRIFT V nanoTOF equipped with a 30 keV Bi_3^{2+} ion gun). The average and maximum flash temperature increases were calculated to be 4 and 12 °C, respectively (see section II in the Supporting Information). The substrate wear was monitored with optical profilometry (Zygo, NewView 7300). In dry N_2, the surface was always worn, even at the lowest load tested in this experiment (0.25 GPa). However, there was negligible wear in the presence of allyl alcohol vapor with $p/p_{sat} \geq 10\%$, as evidenced by no discernible wear mark within the resolution limit of the optical profilometer after removing tribo-polymer products with ethanol rinse (see section I of the Supporting Information).

The MD simulation configuration used to model mechanochemical reactions of allyl alcohol occurring at the sliding interface between two amorphous SiO_2 slabs is shown in Figure 1. The size of the periodic box was 31.9 × 31.9 × 70 Å^3. Instead of the ball-on-flat geometry, a slab-on-slab geometry was used since the curvature of the counter-ball surface is effectively flat at the nanometer length scale of the simulation and this geometry allowed more accurate control of number of molecules being sheared at the interface. The MD simulations consisted of three steps: (i) energy minimization and equilibration, (ii) vertical compression at a 1 m/s speed, and (iii) lateral sliding at a 10 m/s speed for 1 ns. The durations of the equilibration and vertical compression steps were carefully determined for each simulation based

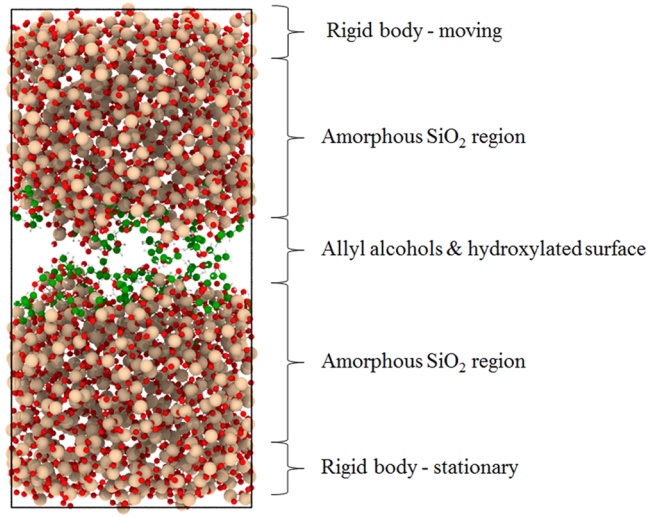

Figure 1. Snapshot of the MD simulation of allyl alcohol sliding between amorphous SiO_2 slabs. The colors of the spheres represent atom types: tan = silicon, red = oxygen, green = carbon, and white = hydrogen.

DOI: 10.1021/acsami.6b14159
ACS Appl. Mater. Interfaces 2017, 9, 3142−3148

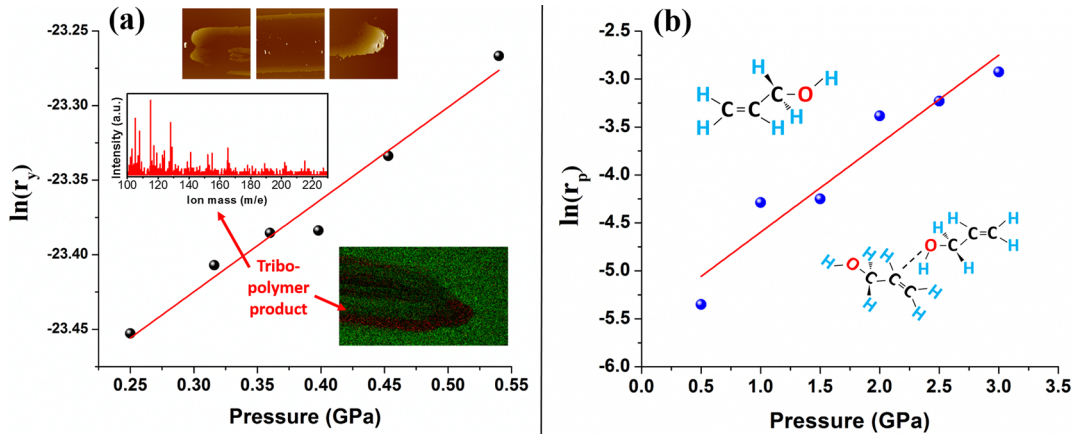

Figure 2. (a) Semilog plot of the tribo-polymer yield (r_y, normalized with the contact area and sliding time) versus applied contact pressure. The synthesis condition was as follows: sliding speed =0.4 cm/s; sliding span and cycle = 2.5 mm and 600 cycles; allyl alcohol vapor = 30% p/p_{sat}; temperature = 295 K. Insets are AFM images of the left, middle, and right regions of a slide track tested at a contact pressure of 0.45 GPa, the mass spectrum of tribo-products from ToF-SIMS analysis, and the selected ion map from ToF-SIMS imaging. (b) Semilog plot of the tribo-polymer production rate (r_p, calculated from the number of molecules containing more than 3 carbon atoms) from MD simulations versus the normal contact pressure. The simulation condition was as follows: sliding speed and time = 10 m/s and 1 ns; number of allyl alcohol molecules = 75; temperature = 300 K. Inset images show the structures of an allyl alcohol molecule and an intermediate forming a dimer.

on the system potential energy and the position of slabs. To evaluate the effect of load on mechanochemical reactions, MD simulations were performed at six different contact pressure (P) conditions: 0.5, 1, 1.5, 2, 2.5, and 3 GPa. Also, to distinguish thermochemical reactions from mechanochemical reactions, additional MD simulations were carried out at temperatures of 300 and 900 K, with no applied load or sliding. In all simulations, 75 molecules of allyl alcohol were included, corresponding to approximately one monolayer of allyl alcohol molecules on the amorphous SiO_2 surfaces. The bottom rigid body region was fixed during all simulations.

All MD simulations used the recently developed ReaxFF force field.[30] Verification of the force field parameters was performed by comparison to density functional theory (DFT) calculations (see Figure S-4 in the Supporting Information). Note that if MD simulations were run with the NVE ensemble (constant number of atoms, volume and energy; i.e., adiabatic condition), then the flash temperature at a sliding speed of 10 m/s would be extremely high. However, the flash temperature at the experimental condition was estimated to be only a few degrees; with the weak temperature dependence of allyl alcohol reactions in the absence of active catalysts (such as cationic initiators), the experimental sliding contact could be assumed to be isothermal. For this reason, simulations were carried under the NVT (constant number of atoms, volume and temperature) ensemble at 300 K. In this case, the frictional heat is dissipated to the heat sink, keeping the simulation temperature at 300 K even at a sliding speed of 10 m/s. For comparison with thermally activated reaction pathways, separate simulations were carried out for the 900 K case without any mechanical compression or shear.

RESULTS AND DISCUSSION

Allyl alcohol molecules physisorbed at the sliding interface can not only provide lubrication effects,[22,31] but they also can react with each other, forming polymeric deposits in and around the slide track.[23] These polymers are often called tribo-polymers. The AFM images shown as insets in Figure 2a show the tribo-polymers piled at both ends of and spread along the slide track. In the VPL experiment, the adsorbed or absorbed allyl alcohol evaporates from the tribo-polymer once the sample is removed from the environment-controlled tribotest cell. This allows chemical analysis of the tribo-polymer, which is one of the main advantages of studying tribochemistry in the VPL condition rather than the liquid-phase lubrication. ToF-SIMS analysis shows ions desorbing from the tribo-polymer areas whose masses are higher than the molecular weight of allyl alcohol (58 amu; inset of Figure 2a). Due to severe fragmentation of organic molecules in ToF-SIMS analysis, the molecular weight distribution of intact polymeric species cannot be determined; but, the presence of ion peaks separated by the mass of CH^+ (13 amu) and CH_2^+(14 amu) are consistent with typical fragmentation patterns of polymeric species. XPS analysis of tribo-polymer products revealed that the atomic ratio of C/O is 3.7 ± 0.2 (see section III in the Supporting Information), which is higher than that of the monomer (3.0). In our previous paper on tribo-reactions of allyl alcohol on stainless steel surfaces, we analyzed the tribo-polymer products with IR.[23] These analyses confirmed the production of polymeric (or oligomeric) species; but, the exact chemical composition or molecular structure cannot be determined from XPS, ToF-SIMS, and IR analyses. It might require NMR analysis, which requires a relative large quantity of sample.

Note that the contact pressure in the ball-on-flat geometry is not constant. It would be ideal to use the flat-on-flat test geometry in experiments; however, a truly constant pressure in the contact region cannot be obtain due to asperity contacts. For this reason, we did not compare the friction force or absolute yield at the same contact pressure condition; instead, the pressure dependence of the tribochemical reaction described by eq 1 is physically more meaningful and can be compared with simulation results. If one wants to compare the effect of different contact geometry in experiments, then the pressure distribution within the contact region should be taken into account. But, as long as the contact geometry is kept constant (as in our experiment), the pressure dependence of the reaction yield is still valid for the purpose of this study.

The tribo-polymerization yield (r_y) could be obtained from the total amount of tribo-polymers imaged with AFM along the slide track. When this yield is plotted on a logarithmic scale against the applied contact pressure (P); a linear relationship with a slope of 0.66 ± 0.04 can be seen clearly (Figure 2a). Since the frictional temperature rise is negligible, the temperature term in eq 1 can be assumed to be constant. If the shear stress (σ) is proportional to P, i.e., $\sigma = \sigma_o + \mu P$, where σ_o and μ are constant,[32] then eq 1 can be simplified as $r_y \propto \exp\left(\frac{\mu \Delta V^*}{k_B T} P\right)$. Then, the slope of the semilog plot of r_y vs P corresponds to $\frac{\mu \Delta V^*}{k_B T}$.

DOI: 10.1021/acsami.6b14159
ACS Appl. Mater. Interfaces 2017, 9, 3142−3148

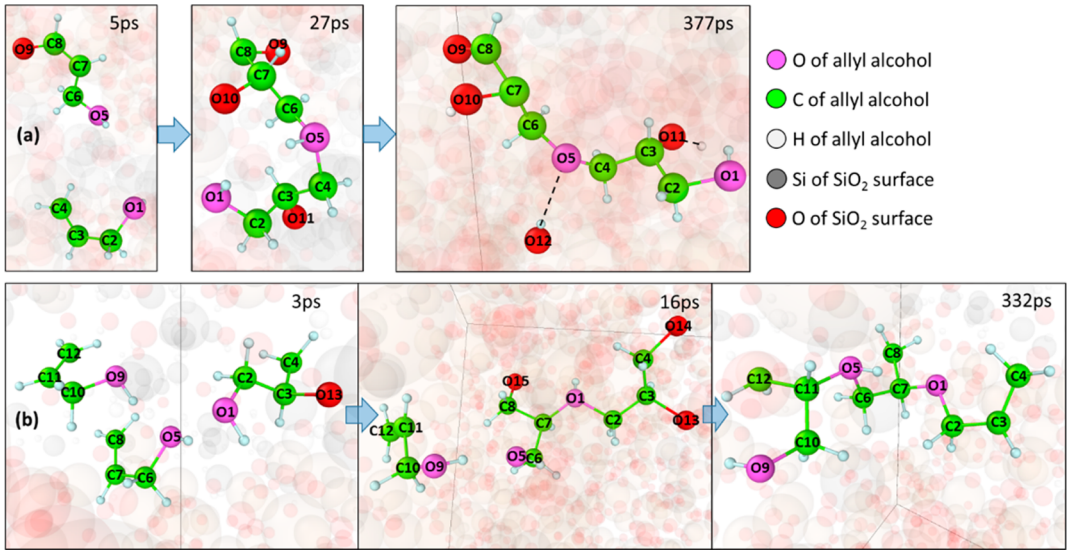

Figure 3. Snapshot images from the ReaxFF simulation showing the association paths of (a) two and (b) three allyl alcohol molecules during sliding at the SiO_2/SiO_2 interface (contact pressure = 1 GPa; slide speed = 10 m/s; temperature = 300 K). Only the atoms involved in mechanochemical reactions are highlighted and numbered for clarification purpose.

In the absence of substrate wear, the constant term μ can be assumed to be the same as the friction coefficient,[22,31,33] which was measured to be ~0.3−0.35 (see Figure S-1 in the Supporting Information). Then, the ΔV^* value for the tribo-polymerization of allyl alcohol at the silicon oxide interface is determined to be 7.8 ± 0.6 Å^3. This value is ~7% of the molar volume of allyl alcohol in the liquid state. Since the molecule is incompressible, the distortion of its volume by ~7% is a significant change. Likely, this is the reason that tribo-polymerization reactions cannot occur at normal conditions without substantial mechanical stress. It should be noted that allyl alcohol is not polymerized readily via a conventional free-radical polymerization mechanism due to the resonant stabilization of allylic radicals.[34,35] Thus, the polymerization of allyl alcohol upon mechanical shear at the tribological interface must occur via pathways that are different from conventional chemical polymerizations.

In order to shed light on the tribo-polymerization mechanisms, we carried out ReaxFF MD simulations of allyl alcohol being sheared at the interface of two amorphous silicon oxide surfaces. Due to computational limitations, MD simulations cannot be performed at the same length and time scales as the experiments. Thus, it is important to verify the relevance between the experimental and computational results by comparing a variable that can be obtained from both approaches. Here, we used the Arrhenius slope of the pressure dependence of tribo-polymerization reaction described by eq 1.

MD simulations showed that allyl alcohol reacts during the slide; the reaction products include chemisorbed species, fragments, and larger molecules formed by association of two or three allyl alcohol molecules. Since the experimental work can detect only the association products with low vapor pressures, we focus on the simulation products with chain lengths longer than three carbons. By fitting the temporal profile of association products with an exponential function (see Figure S-4 in the Supporting Information), we can calculate the reaction rate constant (r_p) at a given contact pressure. When r_p is plotted against P on a semilog plot (Figure 2b), the slope is 0.92 ± 0.13, which is reasonably close to the experimentally determine value (0.66 ± 0.04). This confirms that ReaxFF MD simulation results are relevant to real reactions taking place in the experiment, although the contact load and sliding speed are quite different due to computational limitations.

After confirming the pressure dependence in simulations is comparable with the experimentally observed trend and ruling out microcrack effects as well as frictional heat effects, we can seek mechanistic information from the simulation results to explain the experimental data observed for mechanochemical reactions. In order to compare with thermally activated reactions, simulation results for reactions at 900 K without sliding are also presented in this paper.

Figure 3 displays snapshots of several molecules at various time steps during the sliding simulation, which provides critical information about how allyl alcohol molecules are associated. Figure 3a shows two molecules approaching and reacting with each other. At t = 5 ps, one molecule (C8−C7−C6−O5) is chemisorbed to the surface O9 atom at the C8 position. At t = 27 ps, the O5 atom of that molecule is covalently bonded to C4 of the other molecule. The C3 atom, which was involved in the C═C double bond with C4, is now attached the surface O11 atom. Similarly, C7 is now bonded to the surface O10 atom. At t = 377 ps, the hydrogen attached to O5 is deprotonated and now moved to the surface O12 atom. Figure 3b shows the association of three molecules. Similar to Figure 3a, one molecule (O1−C1−C2−C3) is chemisorbed to the surface O13 atom before the intermolecular reaction. At t = 16 ps, the O1 hydroxyl is covalently bonded to the C7 atom of the second molecule and its double-bond pair C8 is bonded to the surface O16 atom. At t = 332 ps, the O5 hydroxyl group is bonded to the C11 atom of the third molecule and the entire molecule (trimer) is liberated from the surface.

When more molecules were monitored throughout the sliding period, two common features of mechanochemical association reactions were observed. First, one of the reacting molecules is initially chemisorbed at the moving solid surface. It appears that *anchoring one molecule to the surface helps transfer the mechanical force or action from the solid surface to the other molecule being reacted*. This may explain why it is rare to observe the same mechanochemical reactions in static high-pressure conditions without interfacial shear. Second, *the majority of*

DOI: 10.1021/acsami.6b14159
ACS Appl. Mater. Interfaces 2017, 9, 3142−3148

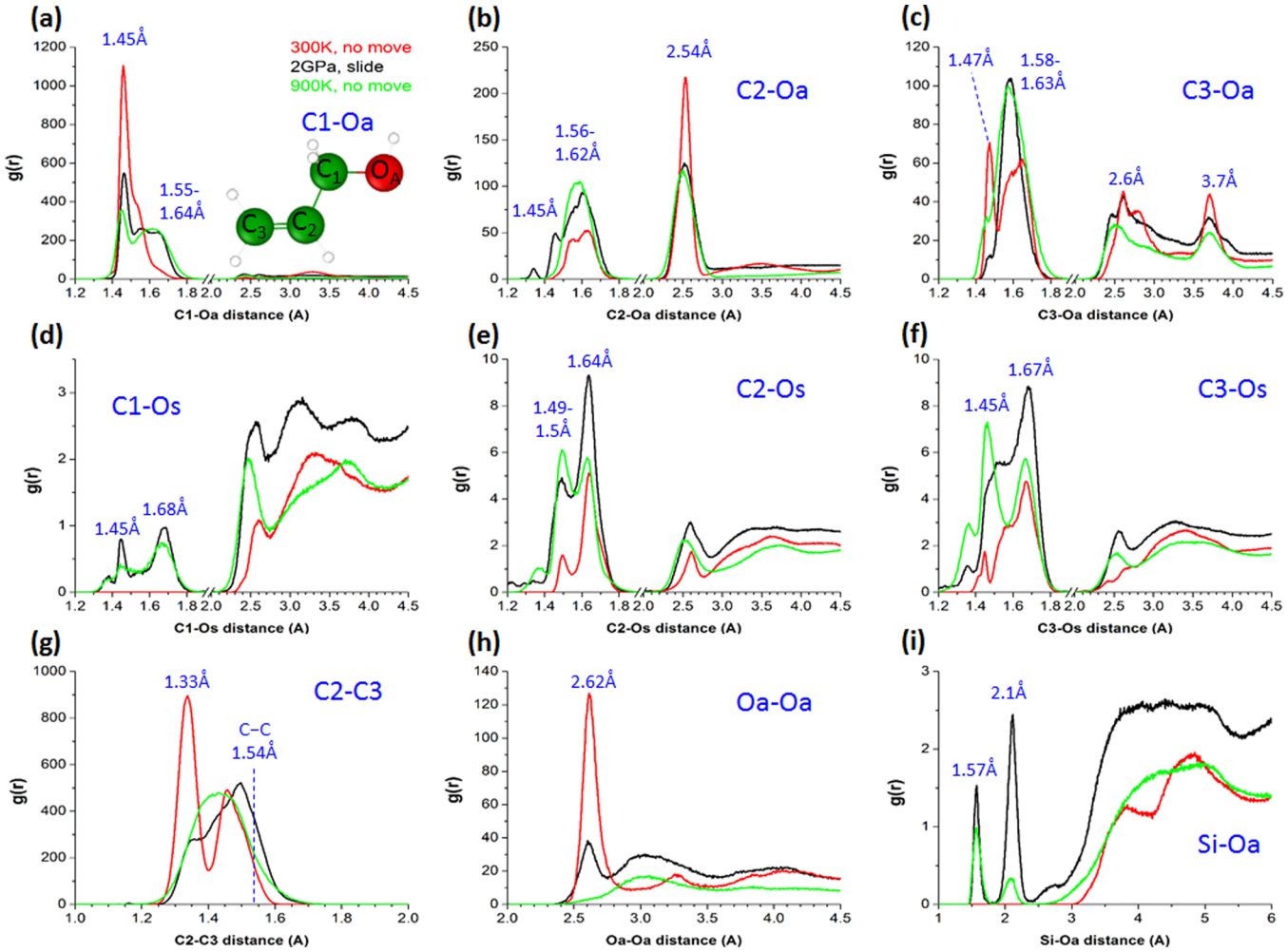

Figure 4. Radial distribution functions (RDFs) for distances between carbon atoms (C1, C2, C3; numbered from OH group, shown as inset to (a)), alcoholic oxygen atoms (Oa), surface oxygen atoms (Os), and silicon atoms (Si) at the interface of silicon oxide. Red curves are at 300 K without load or sliding. Black curves are during the slide (contact load = 1 GPa; slide speed = 10 m/s; temperature = 300 K). Green curves are at 900 K without load or sliding. Each RDF is for a different atom−atom distance: (a) C1−Oa, (b) C1−Oa, (c) C1−Oa, (d) C1−Os, (e) C2−Os, (f) C3−Os, (g) C2−C3, (h) Oa−Oa, and (i) Si−Oa.

chemical bonds leading to association of allyl alcohol molecules are formed between the hydroxyl group of one molecule and one of the carbon atoms in the C═C double bond of another molecule, not between two C═C double bonds as in typical radical polymerization reactions. This is very different from the polymerization reactions of allyl alcohol initiated by Lewis acid catalysts where the carbon radicals are covalently bonded to the carbon atoms of other C═C double bonds.[34,35] More details of the dynamics as well as statistical aspects of mechanochemical reactions can be seen in the radial distribution functions (RDFs) of various pairs of atoms. Figure 4 compares the RDFs of mechanochemical reactions from simulations of sliding at a 2 GPa contact pressure and 300 K with the RDFs of thermal reactions from simulations run at 300 and 900 K without load or sliding.

Figure 4a shows the RDF of the distance between the first carbon atom from the hydroxyl group (C1) and the hydroxyl oxygen (Oa). The main peak at 1.45 Å corresponds to the equilibrium bond length (x_e) for C1−Oa of allyl alcohol.[36] At 300 K without sliding, almost all C1−Oa bonds are populated at this equilibrium distance. As soon as the interface slides, a significant portion of these bonds are elongated to 1.55−1.64 Å; this must be an intermediate state. The critical dissociation length ($x_e + \Delta x^*$) would be at a longer distance than this and would not be observed in an RDF since it is the transition state existing only momentarily. A similar elongation of the C1-Oa length can be seen for the thermal reaction at 900 K.

In the RDFs of C2−Oa and C3−Oa (Figure 4b and c), similar intermediate distances can be seen at 1.56 −1.63 Å. The population of these intermediate states increases upon sliding at 2 GPa or heating to 900 K, compared to the 300 K. It is noted that the covalent bond formation between C2 and Oa of two molecules (1.45 Å) can be seen only for the 2 GPa slide case (Figure 4b). The peak at 2.54 Å in the C2−Oa RDF corresponds to the intramolecular distance between these atoms in one molecule. In the C3−Oa RDF (Figure 4c), the covalent bond formation between these atoms appears to be more likely at 900 K compared to the 2 GPa slide case. Note that at 300 K without sliding, the sharp peak at 1.47 Å in the C3-Oa RDF is longer than typical C−O single bond length (1.43−1.45 Å). This intermediate species is formed due to strong hydrogen bonding interactions, resulting donation of hydrogen from the hydroxyl group to a surrounding oxygen atom (see Figure S-5a in the Supporting Information) and could be an intermediate state unique to the 300 K static state. Again, the two broad peaks centered at ∼2.6 and ∼3.7 Å are the

DOI: 10.1021/acsami.6b14159
ACS Appl. Mater. Interfaces 2017, 9, 3142−3148

intramolecular distances between these atoms in the same molecule. Two values correspond to two different rotational conformers (*gauche* versus *trans* along the C1 sp^3–C2 sp^2 rotational axis).[36]

The surface oxygen (Os) atoms are involved in chemisorption of allyl alcohol molecules. The peaks at 1.49–1.5 Å in the C2–Os RDF (Figure 4e) and 1.45 Å in the C3–Os RDF (Figure 4f) correspond to the covalent bonds between the molecule and the surface oxygen. The C2–Os bond appears to be slightly longer than that of the C3–Os bond; this could be due to steric hindrance of C1 and C3 against the surface. In the 900 K thermal reaction, the propensity of forming covalent bonds with Os seems to be higher at C3 than C2. The small peak at 1.45 Å in the C1–Os RDF (Figure 4d) of the 2 GPa slide case might be formed when the C1 radical is formed by dissociation of the C1-Oa bond during the mechanochemical reactions and compensated by the surface oxygen (Os). The chemisorption probability through the C1–Os bond formation (Figure 4d) appears to be lower than those through the C2–Os and C3–Os sites (Figure 4e and f).

In the C2–C3 RDF (Figure 4g), the sharp peak at 1.33 Å at 300 K is the C=C double bond length.[36] At 300 K, a small fraction of the C=C double bond appears to be elongated to ~1.45 Å; this might be the consequence of the chemisorption of C2 and C3 to the Os site as indicated by a small peak at 1.45 Å in the C2–Os and C3–Os RDFs (Figure 4e and f) or intermolecular interactions between two allyl alcohols (leading to the 1.47 Å in the C3–Oa RDF in Figure 4c). It is noted that, upon interfacial shear at 2 GPa and thermal activation at 900 K, the intact C=C double bond is almost completely disappeared and the distance between these two carbon atoms is elongated to 1.4–1.5 Å. Again, this must be an intermediate state since its distance is shorter than typical length of C–C single bond (1.54 Å).[36]

In the Oa–Oa RDF (Figure 4h), the sharp peak at 2.62 Å corresponds to the O–H···O hydrogen bond. This peak is prominent at 300 K, reduced at the sliding condition, and completely suppressed at 900 K. Since the hydrogen bond is weak, it is not stable at 900 K. In the Si–Oa RDF (Figure 4i), the peak at 1.57 Å must be due to the reaction of alcoholic hydroxyl with the Si dangling bond produced when the surface oxygen (Os) reacts with C2 and C3 of allyl alcohol molecules. This bond is formed only during the mechanical shear or at high temperature conditions and it is not formed in the static condition at 300 K. The peak at 2.1 Å, which is more abundant in the sliding case, is the distance between the hydroxyl group and the undercoordinated silicon (u-Si) atom (see Figure S-5b in the Supporting Information). Those u-Si species reacts with water and allyl alcohol molecules, forming Si–OHs or Si-ORs species during the sliding. The Si-OR species are important here since they are the intermediate species involved in tribo-polymerization reactions (Figures 3 and 4).

With the new insights obtained from ReaxFF MD simulation, we can attempt to interpret the physical meaning of the ~7.8 $Å^3$ value for ΔV^* obtained from the experiments. When we compare the equilibrium C–O bond distance (x_e) and the distances of C–O in the intermediate states, it is clear that Δx^* would be larger than 0.1–0.2 Å along the C–O bond axis. The exact value of Δx^* at the transition state could not be obtained with ReaxFF MD simulations. Let us assume that the upper limit of Δx^* would be comparable to x_e (even though this is unlikely). Then, the critical volume change ΔV^* would be only ~3 $Å^3$ (i.e., cube of the length, 1.45 Å, of the C–O bond that is dissociating or newly forming); obviously, this is much smaller than the experimentally determined value. Thus, a change over a longer distance must be involved. This leads to the premise that *some degree of distortion of the entire molecule from its equilibrium state must occur to activate and initiate mechanochemical reactions*. Such a distortion is possible during *the mechanical shear of molecules covalently anchored to the solid surface by the counter-surface* (Figure 3). This is evidenced by the broadening of the intramolecular distances in the C3–Oa RDFs for the 2 GPa sliding case (Figure 4c).

CONCLUSION

This research explored the mechanistic details underlying tribo-polymerization of allyl alcohol molecules adsorbed and sheared at a silicon oxide interface. A comparison of the Arrhenius slopes of the pressure dependence of tribo-polymerization obtained from experimental measurements and ReaxFF MD simulations verified that atomistic details from the simulations can be used to explain reaction pathways and the physical meaning of the experimentally determined critical activation volume (ΔV^*). It was found that mechanically induced chemical reactions are initiated through distortion of the entire molecule from its equilibrium state, not just single bonds that are being dissociated or formed, and that such structural distortion of molecules is facilitated when molecules are covalently anchored to one of the sliding surfaces.

ASSOCIATED CONTENT

Supporting Information

The Supporting Information is available free of charge on the ACS Publications website at DOI: 10.1021/acsami.6b14159.

Further information and description about flash temperature, XPS analysis result, ReaxFF MD simulation detail and force field validation, and calculation of reaction rate from simulation (PDF)

AUTHOR INFORMATION

Corresponding Author

*E-mail: shkim@engr.psu.edu.

ORCID

Jejoon Yeon: 0000-0001-6323-7572

Seong H. Kim: 0000-0002-8575-7269

Author Contributions

§J.Y. and X.H. contributed equally to this work.

Notes

The authors declare no competing financial interest.

ACKNOWLEDGMENTS

We greatly appreciate National Science Foundation for financial support through the Grant No. CMMI-1435766 and CMMI-1265594.

REFERENCES

(1) Fischer, T. E. Tribochemistry. *Annu. Rev. Mater. Sci.* **1988**, *18*, 303–323.

(2) Hsu, S. M.; Zhang, J.; Yin, Z. The Nature and Origin of Tribochemistry. *Tribol. Lett.* **2002**, *13* (2), 131–139.

(3) Donnet, C.; Belin, M.; Augé, J. C.; Martin, J. M.; Grill, A.; Patel, V. Tribochemistry of Diamond-like Carbon Coatings in Various Environments. *Surf. Coat. Technol.* **1994**, *68–69* (C), 626–631.

(4) James, S. L.; Adams, C. J.; Bolm, C.; Braga, D.; Collier, P.; Friscic, T.; Grepioni, F.; Harris, K. D. M.; Hyett, G.; Jones, W.; Krebs, A.;

DOI: 10.1021/acsami.6b14159
ACS Appl. Mater. Interfaces 2017, 9, 3142–3148

Mack, J.; Maini, L.; Orpen, A. G.; Parkin, I. P.; Shearouse, W. C.; Steed, J. W.; Waddell, D. C.; Friščić, T.; Grepioni, F.; Harris, K. D. M.; Hyett, G.; Jones, W.; Krebs, A.; Mack, J.; Maini, L.; Orpen, A. G.; Parkin, I. P.; Shearouse, W. C.; Steed, J. W.; Waddell, D. C.; et al. Mechanochemistry: Opportunities for New and Cleaner Synthesis. *Chem. Soc. Rev.* **2012**, *41* (1), 413−447.

(5) Baláž, P.; Achimovičová, M.; Baláž, M.; Billik, P.; Cherkezova-Zheleva, Z.; Criado, J. M.; Delogu, F.; Dutková, E.; Gaffet, E.; Gotor, F. J.; Kumar, R.; Mitov, I.; Rojac, T.; Senna, M.; Streletskii, A.; Wieczorek-Ciurowa, K. Hallmarks of Mechanochemistry: From Nanoparticles to Technology. *Chem. Soc. Rev.* **2013**, *42* (18), 7571−7637.

(6) Wang, G.-W. Mechanochemical Organic Synthesis. *Chem. Soc. Rev.* **2013**, *42*, 7668−7700.

(7) Friščić, T.; Halasz, I.; Beldon, P. J.; Belenguer, A. M.; Adams, F.; Kimber, S. a J.; Honkimäki, V.; Dinnebier, R. E. Real-Time and in Situ Monitoring of Mechanochemical Milling Reactions. *Nat. Chem.* **2013**, *5* (1), 66−73.

(8) Wisniak, J. Matches-The Manufacture of Fire. *Indian J. Chem. Technol.* **2005**, *12* (3), 369−380.

(9) Nakayama, K. Triboplasma Generation and Triboluminescence in the Inside and the Front Outside of the Sliding Contact. *Tribol. Lett.* **2016**, *63* (1), 12.

(10) Wasem, J. V.; LaMarche, B. L.; Langford, S. C.; Dickinson, J. T. Triboelectric Charging of a Perfluoropolyether Lubricant. *J. Appl. Phys.* **2003**, *93* (4), 2202−2207.

(11) He, X.; Barthel, A. J.; Kim, S. H. Tribochemical Synthesis of Nano-Lubricant Films from Adsorbed Molecules at Sliding Solid Interface: Tribo-Polymers from α-Pinene, Pinane, and N-Decane. *Surf. Sci.* **2016**, *648*, 352−359.

(12) Gosvami, N. N.; Bares, J. A.; Mangolini, F.; Konicek, A. R.; Yablon, D. G.; Carpick, R. W. Mechanisms of Antiwear Tribofilm Growth Revealed in Situ by Single-Asperity Sliding Contacts. *Science* **2015**, *348* (6230), 102−106.

(13) Adams, H. L.; Garvey, M. T.; Ramasamy, U. S.; Ye, Z.; Martini, A.; Tysoe, W. T. Shear Induced Mechanochemistry: Pushing Molecules around. *J. Phys. Chem. C* **2015**, *119* (13), 7115−7123.

(14) Jacobs, T. D. B.; Gotsmann, B.; Lantz, M. a.; Carpick, R. W. On the Application of Transition State Theory to Atomic-Scale Wear. *Tribol. Lett.* **2010**, *39* (3), 257−271.

(15) Spikes, H.; Tysoe, W. On the Commonality Between Theoretical Models for Fluid and Solid Friction, Wear and Tribochemistry. *Tribol. Lett.* **2015**, *59* (1), 21.

(16) Jacobs, T. D. B.; Carpick, R. W. Nanoscale Wear as a Stress-Assisted Chemical Reaction. *Nat. Nanotechnol.* **2013**, *8* (2), 108−112.

(17) Bell, G. I. Models for the Specific Adhesion of Cells to Cells. *Science* **1978**, *200* (4342), 618−627.

(18) Beyer, M. K.; Clausen-Schaumann, H. Mechanochemistry: The Mechanical Activation of Covalent Bonds. *Chem. Rev.* **2005**, *105* (8), 2921−2948.

(19) Beyer, M. K. The Mechanical Strength of a Covalent Bond Calculated by Density Functional Theory. *J. Chem. Phys.* **2000**, *112* (17), 7307−7312.

(20) Ribas-Arino, J.; Marx, D. Covalent Mechanochemistry: Theoretical Concepts and Computational Tools with Applications to Molecular Nanomechanics. *Chem. Rev.* **2012**, *112* (10), 5412−5487.

(21) He, X.; Kim, S. H. Mechanochemistry of Physisorbed Molecules at Tribological Interfaces: Molecular Structure Dependence of Tribochemical Polymerization. *Langmuir*, **2016**, submitted.

(22) Barthel, A. J.; Kim, S. H. Lubrication by Physisorbed Molecules in Equilibrium with Vapor at Ambient Condition: Effects of Molecular Structure and Substrate Chemistry. *Langmuir* **2014**, *30* (22), 6469−6478.

(23) Barthel, A. J.; Combs, D. R.; Kim, S. H. Synthesis of Polymeric Lubricating Films Directly at the Sliding Interface via Mechanochemical Reactions of Allyl Alcohols Adsorbed from the Vapor Phase. *RSC Adv.* **2014**, *4* (50), 26081−26086.

(24) Yeon, J.; van Duin, A. C. T.; Kim, S. H. Effects of Water on Tribochemical Wear of Silicon Oxide Interface: Molecular Dynamics (MD) Study with Reactive Force Field (ReaxFF). *Langmuir* **2016**, *32* (4), 1018−1026.

(25) Wen, J.; Ma, T.; Zhang, W.; Psofogiannakis, G.; van Duin, A. C. T.; Chen, L.; Qian, L.; Hu, Y.; Lu, X. Atomic Insight into Tribochemical Wear Mechanism of Silicon at the Si/SiO2 Interface in Aqueous Environment: Molecular Dynamics Simulations Using ReaxFF Reactive Force Field. *Appl. Surf. Sci.* **2016**, *390*, 216−223.

(26) Islam, M. M.; Bryantsev, V. S.; van Duin, a. C. T. ReaxFF Reactive Force Field Simulations on the Influence of Teflon on Electrolyte Decomposition during Li/SWCNT Anode Discharge in Lithium-Sulfur Batteries. *J. Electrochem. Soc.* **2014**, *161* (8), E3009−E3014.

(27) Srinivasan, S. G.; Van Duin, A. C. T.; Ganesh, P. Development of a ReaxFF Potential for Carbon Condensed Phases and Its Application to the Thermal Fragmentation of a Large Fullerene. *J. Phys. Chem. A* **2015**, *119* (4), 571−580.

(28) Kim, S. Y.; van Duin, A. C. T.; Kubicki, J. D. Molecular Dynamics Simulations of the Interactions between TiO2 Nanoparticles and Water with Na+ and Cl−, Methanol, and Formic Acid Using a Reactive Force Field. *J. Mater. Res.* **2013**, *28* (3), 513−520.

(29) He, H.; Qian, L.; Pantano, C. G.; Kim, S. H. Mechanochemical Wear of Soda Lime Silica Glass in Humid Environments. *J. Am. Ceram. Soc.* **2014**, *97* (7), 2061−2068.

(30) Chipara, A. C.; Tsafack, T.; Owuor, P.; Yeon, J.; Junkermeier, C. E.; Duin, A. C. T.; Van Bhowmick, S.; Asif, S. A. S.; Brunetto, G.; Douglas, S.; Chipara, M.; Lou, J.; Vajtai, R.; Tiwary, C. S. Amphibious Adhesive Using Solid-Liquid Polymer Mixes. *Science***2016**, submitted.

(31) Asay, D. B.; Dugger, M. T.; Ohlhausen, J. A.; Kim, S. H. Macro- To Nanoscale Wear Prevention via Molecular Adsorption. *Langmuir* **2008**, *24* (10), 155−159.

(32) Carpick, R. W.; Salmeron, M. Scratching the Surface: Fundamental Investigations of Tribology with Atomic Force Microscopy Scratching the Surface: Fundamental Investigations of Tribology with Atomic Force Microscopy. *Chem. Rev.* **1997**, *97* (4), 1163−1194.

(33) Asay, D. B.; Dugger, M. T.; Kim, S. H. In-Situ Vapor-Phase Lubrication of MEMS. *Tribol. Lett.* **2008**, *29* (1), 67−74.

(34) Oh, S. J.; Kinney, D. R.; Wang, W.; Rinaldi, P. L. Studies of Allyl Alcohol Radical Polymerization by PFG-HMQC and HMBC NMR at 750 MHz. *Macromolecules* **2002**, *35* (7), 2602−2607.

(35) Passaglia, E.; Bertoldo, M.; Coiai, S.; Augier, S.; Savi, S.; Ciardelli, F. Nanostructured Polyolefins/Clay Composites: Role of the Molecular Interaction at the Interface. *Polym. Adv. Technol.* **2008**, *19* (6), 560−568.

(36) Kao, J.; Katz, T. Conformational Analysis of Allyl Alcohol. An Ab Initio Molecular Orbital-Study. *J. Mol. Struct.: THEOCHEM* **1984**, *108* (3−4), 229−239.

DOI: 10.1021/acsami.6b14159
ACS Appl. Mater. Interfaces 2017, 9, 3142−3148